EXPERIMENTAL INVESTIGATION OF CRACKING BEHAVIOUR OF CONCRETE BEAMS REINFORCED WITH STEEL FIBRES PRODUCED IN LITHUANIA

Adas Meškėnas[1], Viktor Gribniak[2][✉], Gintaris Kaklauskas[3], Aleksandr Sokolov[4], Eugenijus Gudonis[5], Arvydas Rimkus[6]

Research Laboratory of Innovative Building Structures, Vilnius Gediminas Technical University,
Saulėtekio av. 11, Vilnius, LT–10223, Lithuania
E-mails: [1] adas.meskenas@vgtu.lt; [2] viktor.gribniak@vgtu.lt; [3] gintaris.kaklauskas@vgtu.lt;
[4] aleksandr.sokolov@vgtu.lt; [5] eugenijus.gudonis@vgtu.lt; [6] arvydas.rimkus@vgtu.lt

Abstract. Concrete is the most widely used material for bridge structures in Lithuania. A case study performed by the authors revealed that application of fibres might improve serviceability of such structures. However, adequacy of prediction of the post-cracking behaviour of steel fibre reinforced concrete might be insufficient. The latter issue is closely related to the assessment of the residual strength of steel fibre reinforced concrete. The residual strength, in most cases, is considered as a material property of the cracked concrete. However, in the prediction of the structural behaviour of the concrete members with bar reinforcement, a straightforward application of the residual strength values assessed by using standard techniques might lead to incorrect results. The present study deals with the post-cracking behaviour of structural elements made of concrete with aggregates and fibres provided by Lithuanian companies. Test results of three full-scale and sixteen standard steel fibre reinforced concrete beams with two different content of fibres (23.6 kg/m^3 and 47.1 kg/m^3) are presented. The full-scale beams were reinforced with high-grade steel bars. Effectiveness of the application of the minimum content of the fibres in combination with bar reinforcement was revealed experimentally.

Keywords: bar reinforcement, cracking, reinforced concrete, residual strength, steel fibres, test data.

1. Introduction

Steel fibre reinforced concrete (SFRC) has become a common material in areas such as underground shotcrete structures and industrial floors. The inclusion of fibres into the concrete matrix contributes mainly to the energy absorption capacity and crack control leading to the increased ductility, toughness and post-cracking stiffness of the structural elements (Rafiei *et al.* 2016). Steel fibre reinforcement becomes effective after the concrete cracking initiation and, mostly, improves the post-cracking behaviour, due to the stress transfer mechanisms provided by fibres bridging cracked sections (Gribniak *et al.* 2016). Crack propagation in SFRC is counteracted by the bond stresses induced at the fibres and concrete matrix interface during the fibre pull-out. Therefore, a cracked section is capable to carry tensile stresses. This effect is known as the residual strength of cracked SFRC in tension.

One of the most important properties of SFRC is its ability to transfer tensile stresses across a cracked section. However, it is strongly dependent on the effectiveness of the fibre reinforcement (closely related to fibre geometry, strength, and bond with concrete) as well as fibre orientation and distribution in the cracked section (Vandewalle 2000). SFRC is often considered as a homogenous material. Thus, the ability to resist tension stresses over the cracked section can be described by residual stress-crack opening (σ_{fr}–w) relationship. Residual stresses are determined by using different empirical techniques or experimental methods (uniaxial tension, wedge splitting, bending tests). Due to the difficulties in performing the uniaxial tension and wedge splitting tests, flexural tests on notched beams are widely used for indirect determination of residual stresses in the tension of an SFRC member (Afroughsabet *et al.* 2016). The crack width and the deflection are measured together with the corresponding load applied under deformation control through the flexure layout. The residual strength, consequently, is considered as a material property of the cracked concrete. However, in the prediction of the structural behaviour of the concrete members with bar reinforcement, a straightforward application of the residual strength values assessed by using standard techniques might lead to incorrect results (Deluce *et al.* 2014; Gribniak *et al.* 2012; Sahoo, Sharma 2014; Vandewalle 2000).

Concrete is the most widely used material for bridge structures in Lithuania. Application of fibres might

improve serviceability of such structures (Kaklauskas *et al.* 2014). However, adequacy of prediction of the post-cracking behaviour of SFRC might be insufficient. The present study deals with the post-cracking behaviour of structural elements made of concrete with aggregates and fibres provided by Lithuanian companies. Test results of three full-scale and 16 standard SFRC beams with two different content of fibres (23.6 kg/m³ and 47.1 kg/m³) are presented. The full-scale beams were reinforced with high-grade steel bars. Effectiveness of the application of the minimum content of the fibres in combination with bar reinforcement was revealed throughout the tests.

2. Experimental program

The experimental program consisted of sixteen small (standard) and three full-scale SFRC beams cast using concrete mixtures described in Table 1. The standard specimens were used for assessment of the residual strength of SFRC mixtures *M2* and *M3* with 23.5 kg/m³ and 47.1 kg/m³ of hooked-ended steel fibres (produced by MECHEL NEMUNAS), equivalent to 0.3% and 0.6% of the total concrete volume, respectively. The residual stresses were established according to International Union of Laboratories and Experts in Construction Materials, Systems and Structures (RILEM) and German Committee for Structural Concrete (DAFSTB) recommendations. The respective testing of layouts is shown in Fig. 1.

Three-point bending test according to RILEM was performed on ten 150×150×600 mm prisms. The specimens were notched on one of the faces perpendicular to the casting surface, using wet sawing, through the width of the beam at the midspan. The width and depth of the notch were 5 mm and 25 mm, respectively. The specimens were placed on roller supports assuring a free span of 500 mm. Displacement controlled testing machine was used and beams were loaded with a rate of 0.2 mm/min. The tests were performed under crack tip opening displacement (CTOD) control. For the measurement of CTOD, a linear variable displacement transducer (LVDT) was glued to the specimen and located at the top of the notch. In addition to the CTOD, the deflections on both sides of the beams were measured using LVDT.

Another six small beams were cast and tested following the recommendations of DAFSTB. Four-point bending tests were performed on 150×150×700 mm prisms (a free span of 600 mm). The specimens were tested by using the same testing machine and loading rate as was applied for the RILEM tests, while the DAFSTB tests were performed under deflection control, measuring the deflections on both sides of the beams with LVDTs.

The three full-scale beams had a span of 3000 mm, with a nominal length of 3100 mm or 3280 mm and were tested under a four-point loading scheme. The beams had the same nominal cross-section parameters, resulting in the depth of 300 mm and width of 280 mm (Fig. 2). The beams were reinforced with two 12 mm bars in the tensile zone with the reinforcement ratio of 0.3%. For the top reinforcement two 6 mm bars (reinforcement grade S500) were

used. As shown in Fig. 2, the 6 mm stirrups with 100 mm spacing were used for avoiding shear failure. The beams were made of the concrete containing zero, 23.5 kg/m³ and 47.1 kg/m³ of hooked-ended steel fibres. Main parameters of the full-scale beams are given in Table 2, where A_{s1} and A_{s2} are the cross-section areas of top and bottom reinforcement, respectively; p is the reinforcement ratio of tensile reinforcement; V_f is the volume content of the fibres; f_c is the concrete compressive strength determined by using $\varnothing$150×300 mm cylinders; E_c is the elastic modulus of the concrete; f_y and E_s are the yielding strength and the elastic
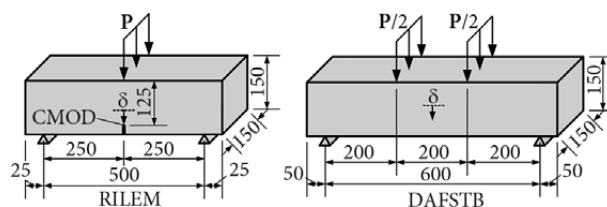
Fig. 1. Specimens and loading schemes of the RILEM and the DAFSTB testing methods of the residual strength
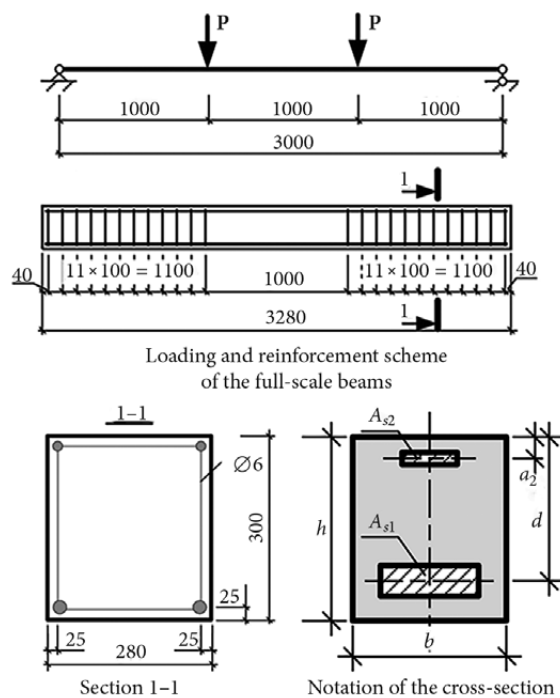
Fig. 2. Loading and reinforcement scheme of the full-scale beams and notation of the cross-section (Table 2 for the Reference)

Table 1. Composition of the concrete mixtures in kg/m³

Mixture	M1	M2	M3
Sand 0/4mm	885	885	885
Crushed aggregate 4/16 mm	975	975	975
Cement CEM I 42.5 N	380	380	380
Concrete plasticizer	1.7	1.7	1.7
Concrete retarder	1.9	1.9	1.9
Water	160	160	160
Fibres MECHEL NEMUNAS	–	23.55	47.10

Table 2. Geometry and material parameters of the full-scale beams

Beam	Concrete mixture	A_{s1}, mm²	A_{s2}, mm²	a_{s2}, mm²	p, %	V_{fb}, %	f_c, MPa	f_s, MPa	E_c, MPa	E_s, MPa
B-1-F0	$M1$	226	56	23	0.3	–	64.47	800.0	40180	194155
B-2-F03	$M2$	226	56	23	0.3	0.3	65.30	800.0	40346	194155
B-3-F06	$M3$	226	56	23	0.3	0.6	62.27	800.0	39767	194155

modulus of the bar reinforcement, respectively. All specimens were cured under the laboratory conditions at average relative humidity (RH) 64.7%. The beams were demoulded in 2–3 days after casting.

The full-scale beams were tested using ПР–1000 testing machine. The load was applied with 2 kN increments only pausing for a short period (approximately 1–2 min) to take readings of the gauge and to measure crack development. The magnitude of the load was fixed using digital 500 kN dynamometer (load cell). The load was applied to the beam through steel traverse (length of traverse is 1250 mm); 10 mm steel plates were glued at the load application place to avoid a stress concentration. The arrangement of the testing equipment is shown in Fig. 3.

The concrete surface strain was measured using 20 mechanical micrometres with circular scale (indicators) with accuracy ±0.003 mm (gauge length is 200 mm). As shown in Fig. 3 (view "A"), four continuous gauge lines (with five mechanical gauges in each line) were located at different heights. The two outer gauge lines were placed along the top and the bottom reinforcement, whereas two other lines were located 60 mm from the boundary lines. The readings of indicators were taken at every load stage. Deflections of the beams were measured with the help of linear variable differential transducers (L_1–L_8, Fig. 3) placed beneath the soffit of each of the beams. The LVDT Almemo T50 with an accuracy of ±0.15% were used for this purpose. The LVDT and dynamometer were connected to a personal computer through signal processing equipment Almemo 25 90–9 and the readings were taken every second.
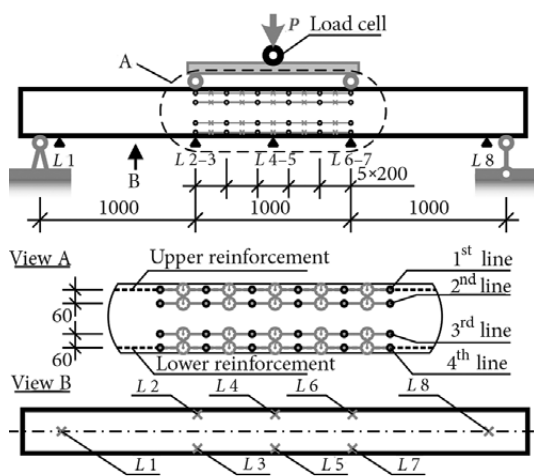
Fig. 3. Structural system and equipment arrangement of the full-scale beams

3. Results and discussion

This section considers the test results of standard and full-scale beams. From the results of individual standard beams tested under three-point loading (Rilem test), load-crack width and load-deflection curves were constructed. Fig. 4 shows the load-crack width diagrams for 0.3% and 0.6% of the volume fibre content (V_f), while Fig. 5 shows the load-deflection diagrams obtained following the DAfStb methodology for 0.3% and 0.6% of fibre content, respectively. Comparative analysis of Figs 4 and 5 reveals two important aspects:

1) Both testing techniques (Rilem and DAfStb) indicate an increase of the peak load and the post-peak load with increased volume of the fibres. This result is quite natural as the increase in the material parameters is related to the number of fibres in a critical section.

2) Scatter in the obtained diagrams is significant, but different for the Rilem and the DAfStb techniques. The testing layout mainly influences such a variety of results. Regardless the loading differences between the three and four point tests, there is a key aspect caused the diverse outcomes: the cross section has a notch at midspan in the three-point bending test, whereas in the four-point bending test the beam is uncut. The DAfStb standard, considering the pure bending zone, "smears" the residual stresses attributing them to the naturally weakest section. Thus, the variation of the section parameters among the samples is less significant as indicated by the Rilem test. Regarding the three-point bending tests, the notch promotes the localization of the crack initiation. Consequently, the residual strength is governed by orientation and number of fibres acting at the pre-notched (unnecessary weakest) section. The arbitrary choice of the notch-place introduces an additional portion of uncertainty into the Rilem test output.

The latter difference in the testing layout causes a variation of the residual strength assessment results. Tables 3 and 4 present the residual strength of the SFRC obtained by the Rilem and the DAfStb methodologies. The strength values (σ_{fr1} and σ_{fr4}) in the tables by both codes are related to the same deflection values, i.e. 0.5 mm and 3.5 mm, respectively. However, these deflections are uneven due to different loading conditions (Fig. 1). Therefore, the residual stress-strain diagrams suitable for the comparison purpose are presented in Fig. 6. For 0.6% fibre content, higher residual stresses are obtained by the DAfStb method, whereas for 0.3% fibre content it shows lower values than the Rilem method. For the same concretes, both approaches indicate the different effect of
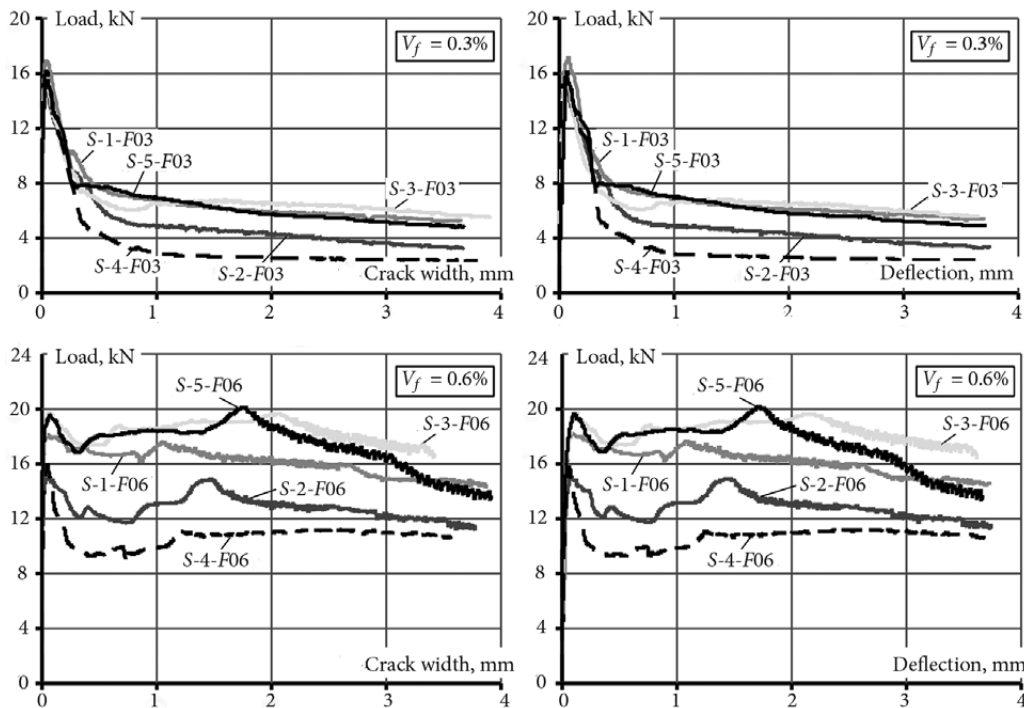
Fig. 4. Load-crack tip opening displacement and load-deflection diagrams of the beams subjected to three-point loading (RILEM test)
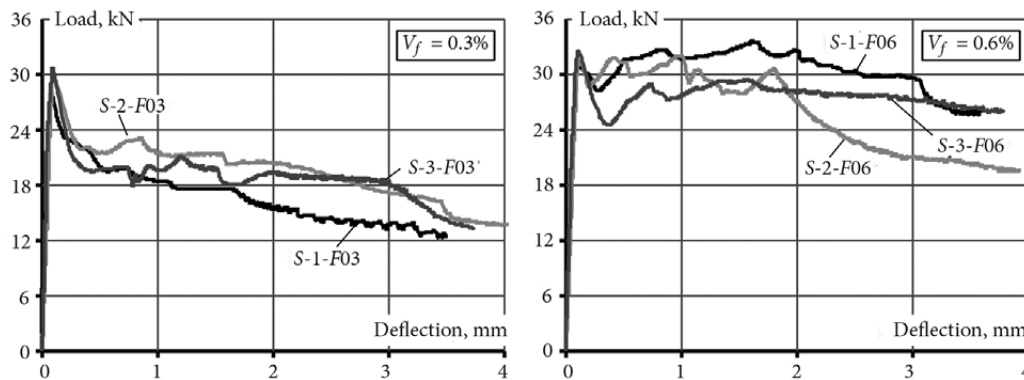
Fig. 5. Load-deflection diagrams of the beams subjected to four-point loading (DAFSTB test)

the increase in the fibre content. Furthermore, the initial strength shown in the diagrams is also different. The initial strength is crucial for the assessment of the fibre effect in the presence of bar reinforcement as the behaviour of such elements is characterized by the increased number of relatively smaller cracks. The disagreement between the RILEM and the DAFSTB models evidences the complexity of the residual strength issue.

The advantage of the four-point un-notched bending (DAFSTB) test is related to the ability of incorporating the effect of variation in the material's strength since the first crack nominally appears at the weakest section. A disadvantage is associated with inability to precede position of the crack. For particular fibre volume ratios and compressive strengths, the formation of several cracks in the pure bending zone complicates measurement of the crack

Table 3. Residual strength of the steel fibre reinforced concrete assessed following the RILEM methodology in MPa

Beam	σ_{fr1}	σ_{fr4}	σ_{fr1}	σ_{fr4}
S-1-F03	1.14	0.66		
S-2-F03	0.92	0.42		
S-3-F03	0.97	0.67	0.96	0.53
S-4-F03	0.65	0.29		
S-5-F03	1.14	0.60		
S-1-F06	2.43	1.73		
S-2-F06	1.79	1.38		
S-3-F06	2.51	2.05	2.13	1.62
S-4-F06	1.36	1.28		
S-5-F06	2.59	1.66		

Table 4. Residual strength of the steel fibre reinforced concrete assessed by following the DAfStb methodology in MPa

Beam	σ_{fr1}	σ_{fr4}	σ_{fr1}	σ_{fr4}
S-1-F03	1.42	0.56		
S-2-F03	1.53	0.68	1.45	0.62
S-3-F03	1.40	0.63		
S-1-F06	2.24	1.15		
S-2-F06	2.22	0.90	2.11	1.07
S-3-F06	1.88	1.17		
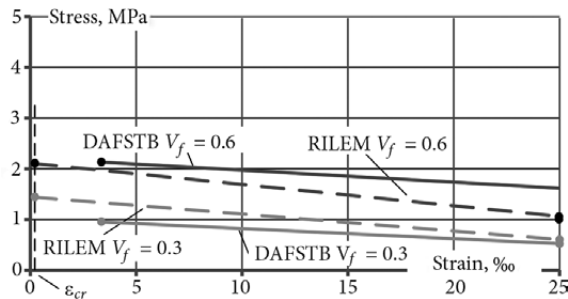
Fig. 6. Residual stress diagrams obtained by the Rilem and the DAfStb methodologies
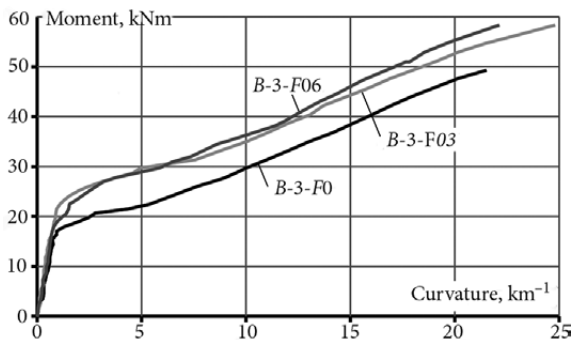
Fig. 7. Experimental curvatures of the steel fibre reinforced concrete beams with bar reinforcement

Fig. 8. The final crack pattern of the full-scale beams

opening and hampers assessment of the deflections (Gopalaratnam 1995). Both approaches, nevertheless, are capable of predicting post-cracking behaviour of SFRC (Blesak *et al.* 2016; Groli, Caldentey 2016; Iqbal *et al.* 2015); however, addition of bar reinforcement complicates assessment of the residual effect of the fibres (Gribniak *et al.* 2012; Sanchez-Aparicio *et al.* 2015).

The moment-curvature relationships of the full-scale beams are shown in Fig. 7. The tests stopped when the ultimate theoretical strain of the high-grade steel reinforcement was reached. Although a significant difference is characteristic of the deformational behaviour of the reference and SFRC beams, the change in the volume of fibres from 0.3% to 0.6% has a marginal effect on the flexural stiffness. Figure 8, presenting the final crack patterns of the test beams, reveals the same tendency – the increase of the fibre content (from 23.5 kg/m^3 to 47.1 kg/m^3) has practically no influence on the crack number. This effect is explained by a relatively small crack width characteristic of the full-scale beams reinforced with longitudinal bars. In other words, the ultimate crack width determined in the full-scale beams at the failure of the bar reinforcement was about 0.2 mm, while the Rilem standard considers 0.5 mm as the minimum characteristic value for assessment of the residual strength. Although the observed crack width of the full-scale beams is related to a particular geometry, material properties, and loading conditions, the cracking range less than 0.5 mm (vital for the assessment of the post-cracking behaviour of SFRC elements with bar reinforcement) is evidently ignored by the standard techniques. Further research is essential to fill this gap in the material science.

4. Concluding remark

The present study is dedicated to the experimental investigation of the post-cracking behaviour of steel fibre reinforced concrete beams made of concrete with aggregates and fibres provided by Lithuanian companies. Test results of three full-scale and sixteen standard steel fibre reinforced concrete beams with two different content of fibres (23.6 kg/m^3 and 47.1 kg/m^3) are presented. The full-scale beams were additionally reinforced with high-grade steel bars. The residual stresses were assessed using the Rilem and the DAfStb methodologies. The results have shown the effectiveness of the minimum content of the fibres in combination with the bar reinforcement for structural applications. Further research should be addressed to the identification of optimal fibre shape and proportions for application in concrete structures with bar reinforcement. Residual strength models of steel fibre reinforced concrete also require modification to cover the range of crack widths less than 0.5 mm.

Acknowledgment

References

Afroughsabet, V.; Biolzi, L.; Ozbakkaloglu, T. 2016. High-Performance Fiber-Reinforced Concrete: a Review, *Journal of Materials Science* 51(14): 6517–6551.
https://doi.org/10.1007/s10853-016-9917-4

Blesak, L.; Goremikins, V.; Wald, F.; Sajdlova, T. 2016. Constitutive Model of Steel Fibre Reinforced Concrete Subjected to

High Temperatures, *Journal of Advanced Engineeering* 56(6): 417–424. https://doi.org/10.14311/ap.2016.56.0417

Deluce, J. R.; Lee, S. C.; Vecchio, F. J. 2014. Crack Model for Steel Fiber-Reinforced Concrete Members Containing Conventional Reinforcement, *ACI Structural Journal* 111(1): 93–102. http://dx.doi.org/10.14359.51686433

Gopalaratnam, V. S. 1995. On the Characterization of Flexural Toughness in Fiber Reinforced Concretes, *Cement and Concrete Composites* 17(3): 239–254.
https://doi.org/10.1016/0958-9465(95)99506-O

Gribniak, V.; Arnautov, A. K.; Norkus, A.; Kliukas, R.; Tamulenas, V.; Gudonis, E.; Sokolov, A. 2016. Steel Fibres: Effective Way to Prevent Failure of the Concrete Bonded with FRP Sheets, *Advances in Materials Science and Engineering* 2016: 1–10. https://doi.org/10.1155/2016/4913536

Gribniak, V.; Kaklauskas, G.; Kwan, A. K. H.; Bacinskas, D.; Ulbinas, D. 2012. Deriving Stress-Strain Relationships for Steel Fibre Concrete in Tension from Tests of Beams with Ordinary Reinforcement, *Engineering Structures* 42: 387–395.
https://doi.org/10.1016/j.engstruct.2012.04.032

Groli, G.; Caldentey, A. P. 2016. Improving Cracking Behaviour with Recycled Steel Fibres Targeting Specific Applications – Analysis According to Model Code 2010, *Structural Concrete* 18(1): 29–39. https://doi.org/10.1002/suco.201500170

Iqbal, S.; Ali, A.; Holschemacher, K.; Bier, T. A. 2015. Mechanical Properties of Steel Fiber Reinforced High Strength Lightweight Self-Compacting Concrete (SHLSCC), *Construction and Building Materials* 98: 325–333.
https://doi.org/10.1016/j.conbuildmat.2015.08.112

Kaklauskas, G.; Gribniak, V.; Bačinskas, D.; Rimkus, A.; Juozapaitis, A.; Misiūnaitė, I.; Tamulėnas, V.; Gudonis, E.; Merkevičius, T.; Garškaitė, A. 2014. *Sumaniųjų tiltų vystymo Lietuvoje galimybių studija, įvertinant išsivysčiusių šalių patirtį* (*Feasibility Study: Development of Smart Bridges in Lithuania Taking into Account the Experience of Developed Countries*), VGTU, 283 p. in Lithuanian

Rafiei, M. H.; Khushefati, W. H.; Demirboga, R.; Adeli, H. 2016. Neural Network, Machine Learning, and Evolutionary Approaches for Concrete Material Characterization, *ACI Materials Journal* 113(6): 781–789.
https://doi.org/10.14359/51689360

Sahoo, D. R.; Sharma, A. 2014. Effect of Steel Fiber Content on Behavior of Concrete Beams with and without Stirrups, *ACI Structural Journal* 111(5): 1157–1166.
https://doi.org/10.14359/51686821

Sanchez-Aparicio, L. J.; Ramos, L. F.; Sena-Cruz, J.; Barros, J. O.; Riveiro, B. 2015. Experimental and Numerical Approaches for Structural Assessment in New Footbridge Designs (SFRSCC–GFPR Hybrid Structure), *Composite Structures* 134: 95–105.
https://doi.org/10.1016/j.compstruct.2015.07.041

Vandewalle, L. 2000. Cracking Behaviour of Concrete Beams Reinforced with a Combination of Ordinary Reinforcement and Steel Fibers, *Materials and Structures* 33(3): 164–170.
https://doi.org/10.1007/BF02479410